Proceedings of the 38th Chinese Control Conference
July 27-30, 2019, Guangzhou, China

Seeking the Scalability in Algebraic Graph Based Unmanned Aerial Vehicle Formation Control

Yu Ding[1], Yirui Cong[1], Xiangke Wang[1], Huiming Li[1]
1. College of Intelligence Science and Technology, National University of Defense Technology, Changsha 410073, P. R. China.
E-mail: xkwang@nudt.edu.cn

Abstract: This paper studies the scalability problem for multi-UAV formation system governed by double-integrator dynamics. More specifically, we focus how to build communication links with fixed control parameters such that the formation can always keep stable when adding arbitrary number of UAVs. A bio-inspired method – Veteran Rule is proposed to solve this problem. Compared to the existing methods, our proposed method does not require to re-design or adaptively adjust the control parameters/gains for the changed Laplacian matrix due to adding new UAVs in the formation system. Furthermore, the optimal convergence rate can be easily designed in our method. Surprisingly, we find that the optimal convergence rate is reached when all the in-degrees equal a particular value, rather than goes unboundedly. Finally, simulation results corroborate the effectiveness of our results.

Key Words: Formation control, scalability, double-integrator, veteran rule, optimal convergence rate.

1 Introduction

Nowadays multiple unmanned air vehicles (UAVs) cooperation is showing its great potential in many civil and military uses [1, 2]. The cooperative UAVs often fly in formation, and algebraic-graph-based formation control is one of two main techniques [3, 4] in supporting the formation flight.[1] Compared to the rigid-graph-based methods, even though the algebraic-graph-based control laws can be easily applied to a 3-dimensional formation and do not have the local minima issue [4], it is faced with the scalability problem. To be more specific, when some UAVs attempt to join the formation system, the Laplacian matrix of the communication topology will change accordingly, but the existing methods cannot handle the scale-changes properly:

- For the control laws relying on the nonzero eigenvalue of the Laplacian matrix (e.g., [6–10]), the design of the control law needs the information of the whole Laplacian matrix to compute eigenvalues, thus the control parameters should be redesigned due to the changes.
- For the fully distributed control laws, a notable method is the adaptive consensus, in which the coupling among agents adjust autonomously to the change of topology. This method overcomes the drawback from utilizing the information of Laplacian matrix (which is to be globally known), e.g., [7–9]. In [11, 12], distributed adaptive protocols were designed to solve linear and nonlinear consensus problems under undirected communication topologies. Since the communication graph are usually asymmetric, [13] then provided a fully distributed solution to the linear consensus problem under directed communication topologies. In [14, 15] adaptive algorithms for switching topologies were proposed. However, for the adaptive consensus based methods, the control gains for other existing UAVs would be affected by the UAVs newly joining the formation system.

Thus, it is necessary to consider the formation scalability problem without changing the control parameters/gains in the whole formation system, i.e., with fixed individual control parameters.

Another important issue for the formation scalability is the convergence rate. Intuitively, the convergence rate can decrease as the number of UAVs changes; and a simple example is for single-integrator systems where the algebraic connectivity varies with the scale of the formation system. Hence, the convergence rate in the formation scalability problem is a meaningful and essential topic to study.

In this work, we use the double-integrator model to serve as the first step towards studying the scalability in UAV formation control systems. We note that the convergence rate cannot only be guaranteed but also be designed in an optimal way. The main contributions are given as follows:

- A method inspired from pigeon formations to build interaction topology is proposed, and we call it the Veteran Rule. It is shown that when using the Veteran Rule, the system can always have the formation stability with system scalability, and the control parameter in each UAV is fixed.
- The convergence rate of the system under the Veteran Rule is analyzed. Surprisingly, the convergence rate of the system reaches maximum value when all the in-degrees equal a particular value, rather than goes unboundedly. Based on this result, the Veteran Rule with optimal convergence rate is proposed.

Section 2 gives the system model and the problem description. In Section 3, we propose the Veteran Rule to guarantee the formation scalability where the rigorous proof is given. Furthermore, convergence rate is analyzed and its optimal design is provided in Section 4. In Section 5, simulation results corroborate the effectiveness of our methods. Finally, the concluding remarks are given in Section 6.

2 System Model and Problem Description

2.1 Basic Concepts In Graph Theory

To present problem description, some basic concepts in graph theory related to our work are briefly summarized in

This work is partially supported by National Natural Science Foundation (NNSF) of China under Grant 61801494.

The corresponding author is Xiangke Wang.

[1]The other main technique in formation control is based on rigid graph [5].

this subsection.

A directed graph $\mathcal{G}$ can be described by a triple $(\mathcal{V}, \mathcal{E}, \mathcal{W})$, where $\mathcal{V} = \{1, \ldots, N\}$ is the node set, and $\mathcal{E} \subseteq \mathcal{V} \times \mathcal{V}$ denotes the edge set, and $\mathcal{W} = [w_{ij}] \in \mathbb{R}^{N \times N}$ with $w_{ij} \geq 0$ represents the adjacency matrix such that $(i, j) \in \mathcal{E}$ if and only if $w_{ji} > 0$. In this work, we assume $\mathcal{G}$ is simple (i.e., with no self-edges), which means $w_{ii} = 0$ for all $i \in \mathcal{V}$. The set of neighbors of node i is denoted by $\mathcal{N}_i = \{j \in \mathcal{V} : (j, i) \in \mathcal{V}\}$. The in-degree of the node i is defined by $\deg_{\text{in}}(i) = \sum_{j \in \mathcal{N}_i} w_{ij}$, and the degree matrix is $\mathcal{D} = \{\deg_{\text{in}}(1), \ldots, \deg_{\text{in}}(N)\}$. With the adjacency matrix $\mathcal{W}$ and the degree matrix $\mathcal{D}$, we can define the Laplacian matrix $\mathcal{L}$ of $\mathcal{G}$ by $\mathcal{L} = \mathcal{D} - \mathcal{W}$. A directed path from i to j is a sequence of ordered edges of the form $(i, k_1), (k_1, k_2), \ldots, (k_l, j)$, and we say $\mathcal{G}$ has a spanning tree if at least one node has a directed path to the other nodes. The following lemma gives some basic properties of the Laplacian matrix $\mathcal{L}$.

Lemma 1 ([16]). *Let $\mathcal{L} \in \mathbb{R}^{N \times N}$ be the Laplacian matrix of a directed graph $\mathcal{G}$ and $\mathbf{1}_N = [1, 1, \ldots, 1]^T \in \mathbb{R}^N$, then*

i) $\mathcal{L}$ at least has a zero eigenvalue, and $\mathbf{1}_N$ is the associated eigenvector, that is $\mathcal{L}\mathbf{1}_N = 0$;

ii) If $\mathcal{G}$ has a spanning tree, then 0 is a simple eigenvalue of $-\mathcal{L}$, and all the other $N-1$ eigenvalues of $-\mathcal{L}$ have negative real-parts.

2.2 System Model

Consider a group of N UAVs with local communications. A directed graph $\mathcal{G}$ can be used to describe the communication topology of the formation system. More specifically, node $i \in \mathcal{V}$ stands for the i^{th} UAV, and edge $(i, j) \in \mathcal{E}$ represents the communication link from UAV i to UAV j whose strength is denoted by w_{ji}. All the UAVs move in d-dimensional space ($d \in \{2, 3\}$), and we let $\xi_i(t) \in \mathbb{R}^d$ and $\zeta_i(t) \in \mathbb{R}^d$ be the position and velocity states of UAV i, respectively. We assume the autopilot is properly designed such that the dynamics of each UAV i satisfies:

$$\begin{cases} \dot{\xi}_i = \zeta_i, \\ \dot{\zeta}_i = u_i, \end{cases} \tag{1}$$

where the input $u_i \in \mathbb{R}^d$ is the acceleration of UAV i which can be timely controlled. In this work, we need all the UAVs achieve a given formation pattern and share the same speed. Here we consider the consensus-based formation controller as follows

$$u_i = -\sum_{j \in \mathcal{N}_i} w_{ij}[(\xi_i - \xi_j - \Delta_{ij}) + \gamma(\zeta_i - \zeta_j)], \tag{2}$$

where $\Delta_{ij} = \Delta_i - \Delta_j$ denotes the desired relative position of UAV i w.r.t. UAV j; and Δ_i (Δ_j) is the offset of UAV i (UAV j) determined by the formation pattern; and $\gamma > 0$ is a parameter. By setting $\xi = [\xi_1, \xi_2, \ldots, \xi_n]$, $\zeta = [\zeta_1, \zeta_2, \ldots, \zeta_n]$, and $\widehat{\xi} = [\xi_1 - \Delta_1, \xi_2 - \Delta_2, \ldots, \xi_n - \Delta_n] =: \xi - \Delta$, the closed-loop system with (1) and (2) can be written as

$$\begin{bmatrix} \dot{\widehat{\xi}} \\ \dot{\zeta} \end{bmatrix} = \Gamma \otimes I_d \begin{bmatrix} \widehat{\xi} \\ \zeta \end{bmatrix}, \tag{3}$$

where

$$\Gamma = \begin{pmatrix} 0 & I_{N \times N} \\ -\mathcal{L} & -\gamma\mathcal{L} \end{pmatrix}. \tag{4}$$

Note that system (3) simplifies the analysis of the formation stability defined in Definition 1.

Definition 1 (Formation stability). *We say system* (1) *achieves formation stability, if $\xi_i - \xi_j \to \Delta_{ij}$ and $\zeta_i - \zeta_j \to 0$ as $t \to \infty$.*

Remark 1. *In Definition 1, $\xi_i - \xi_j \to \Delta_{ij}$ means $\|\widehat{\xi}_i - \widehat{\xi}_j\| \to 0$, which further implies system* (3) *achieves consensus. Thus, for all $i \in \{1, \ldots, N\}$, the following equation holds*

$$\lim_{t \to \infty} \left\| \begin{bmatrix} \widehat{\xi} \\ \zeta \end{bmatrix} - c(t) \otimes \mathbf{1}_N \right\| = 0, \tag{5}$$

where $c(t)$ is called the consensus state trajectory or consensus function [16].

With $c(t)$, we can define the formation error as

$$\delta(t) = \begin{bmatrix} \xi - \Delta \\ \zeta \end{bmatrix} - c(t) \otimes \mathbf{1}_N, \tag{6}$$

whose asymptotic convergence is equivalent to that in (5).

Next, we define the convergence rate of formation error as follows.

Definition 2 (Convergence Rate). *The convergence rate of the formation error $\delta(t)$ is the largest exponent β^* to exponentially bound $\|\delta(t)\|$[17], i.e.,*

$$\beta^* = \max\{\beta > 0 \colon \|\delta(t)\| \leq \alpha(\|\delta(0)\|)e^{-\beta t}\}, \tag{7}$$

where $\alpha(\cdot)$ is a class $\mathcal{K}$ function [18].

2.3 Problem Description

In this paper, we study the scalability problem for formation control that without changing control parameter γ. To be more specific, how to design the communication links as well as their strengths such that:

i) The formation system is still stable after adding new UAVs, i.e., the system has scalability (see Problem 1);

ii) Furthermore, the convergence rate of the formation error is maximized (see Problem 2).

Note that the scalability does not intrinsically hold in formation systems. When adding new UAVs, the same control parameter γ cannot always maintain the formation stability, if the communication links and their strengths are not properly designed. The following proposition gives the necessary and sufficient condition for the formation stability, which well explains why γ is correlated to the scale of formation system.

Lemma 2 ([19]). *Assume that the interaction topology $\mathcal{G}$ has a spanning tree. Let μ_i denote the i^{th} eigenvalue of $-\mathcal{L}$. $\text{Re}(\mu_i) = p_i$ and $\text{Im}(\mu_i) = q_i$ are the real and imaginary parts of μ_i, respectively. Then the system* (1) *achieves formation stability (see Definition 1) if and if only*

$$\gamma > \max_{2 \leq i \leq N} \frac{q_i}{\sqrt{|p_i||\mu_i|}}. \tag{8}$$

From Lemma 2, we can see that a formation stable γ is constrained by the communication links and their strengths (through the Laplacian matrix $\mathcal{L}$). Consider a formation system with N UAVs which has reached formation stability. Assume M new UAVs join in this system, and they will build communication links to the original N UAVs, which makes the Laplacian matrix $\mathcal{L}$ extend to $(N+M)^2$ dimensions. The new entries will change the original N eigenvalues, and also bring new M eigenvalues. This means the originally satisfied condition (8) is fragile after adding new UAVs. Thus, it is necessary to study the scalability problem in formation control systems, which is formally defined in Problem 1.

Problem 1. *Assume the formation system with $N \geq 1$ UAVs is formation stable (see Definition 1). After adding arbitrary $M \geq 1$ UAVs but without changing γ, how to build new communication links to these M UAVs such that the new formation system with $N + M$ UAVs is still formation stable?*

Furthermore, it is important to optimize the convergence rate of the formation error $\delta(t)$, which is given in Problem 2.

Problem 2. *Based on Problem 1, how to design the strengths w_{ij} for these newly built communication links such that the convergence rate β^* (see Definition 2) is maximized?*

3 The Veteran Rule and Formation Scalability

3.1 The Veteran Rule

In nature we often see pigeons flying in a flock. Even though sometimes several separated individuals will join the flock, but the flock still maintains its formation and keeps stable. So analyzing the behavior model of pigeons may give us some inspiration to solve the formation scalability problem. In this section, we will show a interaction basic rule that we found among pigeons, which we call it "Veteran Rule". According to this rule, we build an interaction topology, and we will show that with this kind of topology the system can always achieve formation stability with system scalability.

Through the study of pigeon flocks, we have a conclusion that experienced pigeons tend to fly in front of the flock, while unexperienced pigeons tend to fly in latter of the flock [20]. Based on this, we call the pigeon with more navigation experience in a pair the "leader" and the other with less experience the "follower". It is found that the leader always tends to take the position of front while the follower tends to fly in latter of the leader [21]. Through visual information, followers can respond (usually copy and imitate) to the behaviour of the leader [22], thus followers will be able to accomplish their homing or migration [23]. However, the followers are in leaders' blind spots so that whatever followers do, leaders cannot perceive their behavior, thus will not make any response [24]. We call this rule the "Veteran Rule" that the information transfer is only from experienced individuals to unexperienced individuals, or we say unexperienced individuals only obtain unidirectional information from experienced individuals.

3.2 Formation Scalability

For UAVs, we define a Q value $Q(i)$ similar to the experience of pigeons in the flock for each agent i in the system. $Q(i)$ can be defined in any arbitrary way as long as for any two agents their Q values can be compared.

Theorem 1 (System Scalability)**.** *Assume that the interaction topology $\mathcal{G}$ has a spanning tree, when information only flows from high value agents to low value agents, the system always achieves formation stability with scalability (see Problem 1).*

Proof. This proof is divided into two steps. In the first step, we prove that the communication topology built according to the Veteran Rule corresponds to a directed acyclic graph. Then in the second step, we prove the formation stability with scalability.

Firstly, to prove the graph is a directed acyclic graph, we only need to prove for any node i and j when there is a directed path from i to j, there is never a directed path from j back to i. We consider the experience of individual i as a function $Q(i)$ of i. When there is a directed path from the node i to node j, we have $Q(i) > Q(j)$. Next we will prove there is never a directed path from j to i by contradiction. Assume there is a directed path from j to i that passes $j, j_1, \ldots, j_k, i$, which implies $Q(j) > Q(j_1) > \cdots > Q(j_k) > Q(i)$. This contradicts $Q(i) > Q(j)$. Thus there is never a directed path from j back to i for any two given nodes i and j, and the graph is a directed acyclic graph.

Secondly, we show the system achieve formation stability with scalability. Denote the elementary matrix that exchanges the i^{th} row and the j^{th} row as P_{ij}. For any adjacency matrix corresponding to a directed acyclic graph W, denote $U = P_{i_1 1} P_{i_2 2} \cdots P_{i_N N}$, where $i_1, i_2, \cdots, i_N$ are the nodes of the system whose Q values are ranked in a decreasing order. System (3) can be linearly transformed by $\begin{bmatrix} \widetilde{\xi} \\ \widetilde{\zeta} \end{bmatrix} = U \begin{bmatrix} \widehat{\xi} \\ \zeta \end{bmatrix}$, and the transformed adjacency matrix $W^* = U^{-1} W U$ satisfies for any $i < j$, for $Q(i) > Q(j)$, $w^*_{ij} = 0$. So the adjacency matrix and the Laplacian matrix of the system is a lower triangular matrix.[2] The eigenvalues of the Laplacian matrix μ_i is a real negative number, i.e., $q_i = \mathrm{Im}(\mu_i) = 0$. This implies the necessary and sufficient condition (8) in Lemma 2 becomes $\gamma > 0$. Thus the system achieves formation stability. Since N can be an arbitrary number, the conclusion holds when the number of the formation is $N + M$. □

4 Convergence Rate Analysis

Convergence rate is an important performance index of a system. In this section, we consider the convergence rate maximization problem (i.e., Problem 2) under the Veteran Rule.

Intuitively speaking, it seems that larger in-degrees lead to a higher convergence rate, since they represent the connection strengths in a network. However, in this section, we show that the in-degrees are not the larger the better, and the maximum convergence turns out to be achieved when all the in-degrees are equal to a particular value. This result is given in Theorem 2.

Theorem 2 (Optimal Convergence Rate)**.** *The convergence rate of the swarm system achieves maximum when the in-*

[2] Another method to prove the Laplacian matrix corresponding to a directed acyclic graph can be transformed into a lower triangular matrix is shown in [10].

degree of every node equals $\frac{4}{\gamma^2}$. The optimal convergence rate is $\frac{2}{\gamma}$.

Proof. Without loss of generality, we assume the UAVs are ranked in the topological order, and the in-degrees of nodes d_i satisfy $d_2 \leq d_3 \leq \cdots \leq d_N$. For the Laplacian matrix $\mathcal{L}$ is a lower triangular matrix, the in-degree of each node $d_i = -\mu_i$. Denote $\lambda_{i_+} = \frac{\gamma\mu_i + \sqrt{\gamma^2\mu_i^2 + 4\mu_i}}{2}$ and $\lambda_{i_-} = \frac{\gamma\mu_i - \sqrt{\gamma^2\mu_i^2 + 4\mu_i}}{2}$. The convergence rate of the system is determined by $\max_{2\leq i\leq N} \mathrm{Re}(\lambda_i)$, and for each μ_i the corresponding $\lambda_{i\pm}$ always have $\mathrm{Re}(\lambda_{i-}) \leq \mathrm{Re}(\lambda_{i+})$. So when analyzing the convergence rate, we just need to consider all the λ_{i+}. To analyze the variation of λ_i, we draw the parameter root locus of λ when μ varies from 0 to $-\infty$ (see Fig. 1), it is not hard to prove the root locus forms a circle described by $(x + \frac{1}{\gamma})^2 + y^2 = \frac{1}{\gamma^2}$, where $x,\ y$ denote the imaginary and real part, respectively. Since $|\mu_2| \leq |\mu_3| \leq \cdots \leq |\mu_N|$, we know that $\lambda_{i+}(\mu_i)$ $(i = 3, 4, \ldots, N)$ runs in front of $\lambda_{2+}(\mu_2)$ along the root locus. Through the root locus we know that (see figure 1)$\lambda_- \to -\infty$ as $\mu \to -\infty$, and $\lambda_+ \to -\frac{1}{\gamma}$ as $\mu \to -\infty$. $\mathrm{Re}(\lambda)$ reaches it minimum at the right endpoint of the circle (noted with a triangle in Fig. 1), moving forward along the root locus, λ_+ runs on the real axis from $-\frac{2}{\gamma}$ to $-\frac{1}{\gamma}$. Thus we have

$$\beta^* = \max \mathrm{Re}(\lambda_{\mu_{i_+}}) = \max\{\mathrm{Re}(\lambda_{\mu_{2_+}}), \mathrm{Re}(\lambda_{\mu_{N_+}})\}. \quad (9)$$

When $\mathrm{Re}(\lambda_{\mu_{2_+}}), \mathrm{Re}(\lambda_{\mu_{N_+}})$ simultaneously reaches their minimum, the system converges at the maximum rate. Thus the optimal situation is all the λ_{i_+} lie on the right endpoint of the circle. By this time, $\beta^* = \lambda_{i_2} = \lambda_{i_N} = -\frac{2}{\gamma}$, which implies $\mu_{i_2} = \mu_{i_N} = -\frac{4}{\gamma^2}$. Thus the in-degree $d_i = \frac{4}{\gamma^2} \quad i = 2, 3, \ldots, N$. □

So the in-degree of all the nodes should align close to $\frac{4}{\gamma^2}$, and larger or smaller in-degrees will bring the loss of convergence rate. For UAVs with high $Q(i)$ values, their number of connections are small, to satisfy their in-degree lie close to $\frac{4}{\gamma^2}$, and their weight of interaction topology w_{ij} should be larger. The UAVs with low $Q(i)$ values have more choices of the agents they build connection with, to control their in-degree, these UAVs just need to choose part of their connectable UAVs.

Remark 2. *If the control parameter γ decreases, the optimal convergence rate $\frac{2}{\gamma}$ increases and thus the system achieves formation stability with a higher convergence rate. One may ask with the input form* (2)*, it seems like a contradiction when γ tends to 0, the gain decreases while the convergence rate of the system increases. In fact, the in-degree of the node is $\sum_{j=1}^{n} w_{ij}$. If we assume w_{ij} is proportional to the in-degree of the node, i.e., $w_{ij} \propto \frac{4}{\gamma^2}$, then the control gains of $\xi_i - \xi_j - \Delta_{ij}$ and $\zeta_i - \zeta_j$ are proportional to $\frac{1}{\gamma^2}$ and $\frac{1}{\gamma}$, respectively. Thus, as γ decreases, the control gains increase, which coincides with a larger convergence rate.*

5 Simulation

This section contains two subsections. In Section 5.1, we corroborate the effectiveness of our proposed Veteran Rule in formation scalability, where the formation systems with 12 and 600 UAVs are considered, respectively. In Section 5.2, our theoretical results in the optimal convergence rate are verified.

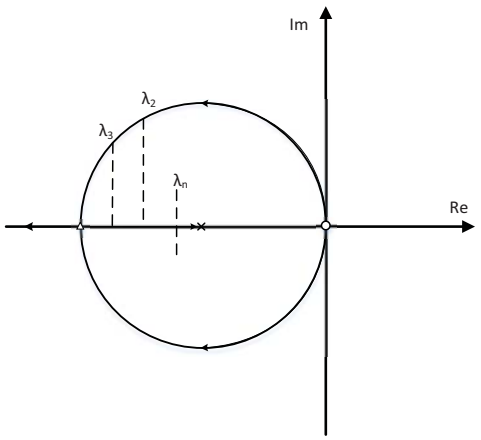

Fig. 1: The root of polynomial $\lambda^2 - \lambda\mu\gamma - \mu$ when μ varies from 0 to $-\infty$. The root locus begins from 0, $\mathrm{Re}(\lambda)$ in the beginning decreases along the circle $(x + \frac{1}{\gamma})^2 + y^2 = \frac{1}{\gamma^2}$ to $-\frac{2}{\gamma}$, as the variation of μ continues, λ lies on the negative part of the real axis, λ_- tends to $-\infty$ while λ_+ tends to $-\frac{1}{\gamma}$. The eigenvalues of the Laplacian matrix μ_i have an order of $|\mu_{i_2}| \leq |\mu_{i_3}| \leq \cdots \leq |\mu_{i_N}|$. $|\mu_{i_2}| \leq |\mu_{i_3}| \leq \cdots \leq |\mu_{i_N}|$, $\lambda_{i+}(\mu_i)$ $i = i_3, i_4, \ldots, i_N$ runs in front of $\lambda_{i_{2+}}(\mu_{i2})$ along the root locus. So $\min|Re(\lambda_{\mu_{i_+}})| = \min|Re(\lambda_{\mu_{i_{2_+}}})|, |\lambda_{\mu_{i_{N_+}}}|$.

5.1 The Veteran Rule

To demonstrate the effectiveness of The Veteran Rule in UAV formation, a 10 UAV formation system with 2 new joining UAVs is considered. The adjacency matrix of the 10 UAV system is

$$W = \begin{bmatrix} 0 & 0 & \cdots & \cdots & \cdots & \cdots & \cdots & \cdots & \cdots & 0 \\ 6 & 0 & \cdots & \cdots & \cdots & \cdots & \cdots & \cdots & \cdots & 0 \\ 3 & 5 & 0 & \cdots & \cdots & \cdots & \cdots & \cdots & \cdots & 0 \\ 3 & 2 & 3 & 0 & \cdots & \cdots & \cdots & \cdots & \cdots & 0 \\ 4 & 3 & 5 & 4 & 0 & \cdots & \cdots & \cdots & \cdots & 0 \\ 4 & 3 & 3 & 3 & 3 & 0 & \cdots & \cdots & \cdots & 0 \\ 0 & 0 & 0 & 5 & 5 & 3 & 0 & \cdots & \cdots & 0 \\ 0 & 0 & 0 & 0 & 4 & 4 & 5 & 0 & \cdots & 0 \\ 2 & 0 & 3 & 2 & 1 & 3 & 2 & 2 & 0 & 0 \\ 0 & 0 & 0 & 2 & 3 & 2 & 1 & 2 & 3 & 0 \end{bmatrix}, \quad (10)$$

and the control parameter is $\gamma = 0.1$. Assume the UAVs are ranked in the reverse order of their Q values, which implies $Q(1) > Q(2) > \cdots > Q(10)$. The communication topology as well as the formation pattern of the system are shown in Fig. 2(a) and the 10 UAV system finally forms a circle pattern [see Fig. 2(b)]. Without loss of generality, we assume the two joining UAVs' Q values satisfy $Q(12) < Q(11) < Q(10)$, and the relative positions for UAVs 11 and 12 are $\Delta_{11} = [0, -10]^T$ and $\Delta_{12} = [-16.1803, 11.7557]^T$, respectively [see Fig. 2(a)]. When using the Veteran Rule, the adding edges in the topology are $w_{11,2} = 3$, $w_{11,5} = 2$, $w_{11,6} = 3$, $w_{11,7} = 2$, $w_{11,9} = 3$, $w_{11,10} = 2$, $w_{12,7} = 2$,

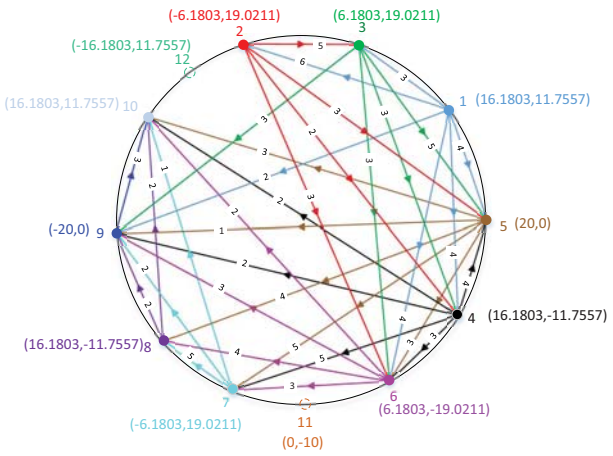

(a)

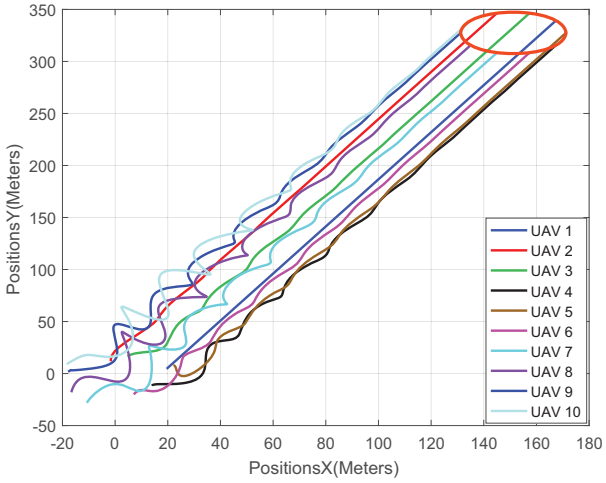

(b)

Fig. 2: The UAVs are ranked in the reverse order of their Q values, $Q(1) > Q(2) > \cdots > Q(10)$, and the 10 UAVs system finally goes forward in a shape of circle. (a) Communication topology and formation pattern of the 10 UAV formation system (e.g., $(5, 20)$ means $\Delta_5 = [5, 20]^T$), where we also label UAVs 11 and 12 (new UAVs to join the formation system) using dashed circles. (b) 10 UAVs achieve formation stability and form the expected circle pattern.

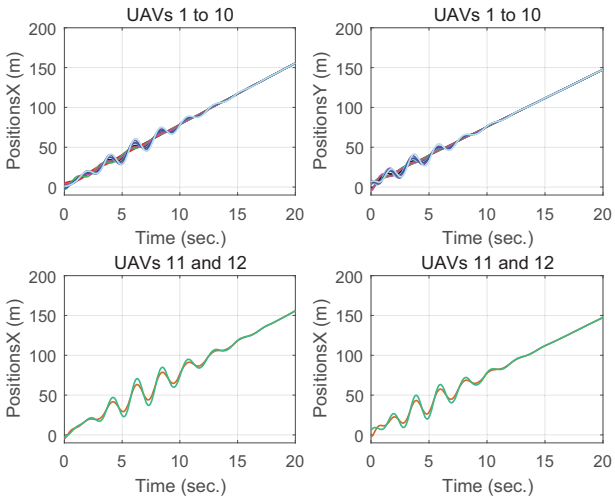

(a)

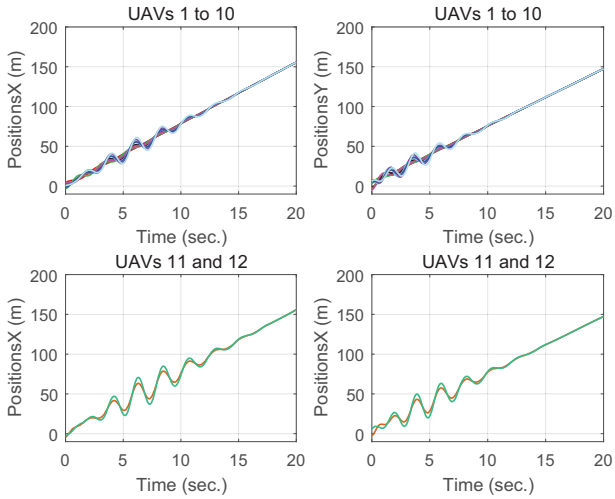

(b)

Fig. 3: Two new UAVs using the Veteran Rule join in the flock. After a short period of oscillation, the system reaches formation stability. (a) Position curves of the formation system; (b) Velocity curves of the formation system.

$w_{12,8} = 3$, and $w_{12,9} = 4$. By Theorem 1, the system will finally achieve formation stability, and the response curves of $\widehat{\xi}$ and ζ are as shown in Fig. 3(a) and Fig. 3(b), respectively.

Next we will give an example as an comparison that the new two UAVs build connections without the Veteran Rule. Besides the edges coincide with the Veteran Rule we mentioned above, some more edges are also added in the topology: $w_{3,11} = 1$, $w_{4,11} = 2$, $w_{6,11} = 1$, $w_{8,11} = 1$, $w_{9,11} = 1$, $w_{10,11} = 2$, $w_{4,12} = 2$, $w_{7,12} = 2$, $w_{8,12} = 1$, $w_{9,12} = 2$, $w_{10,12} = 1$, and $w_{11,12} = 6$. One of the eigenvalues of the new Laplacian matrix is $\mu = -12.8136 \pm 5.5.328i$, $p = \mathrm{Re}(\mu) = -12.8136$, $q = \mathrm{Im}(\mu) = 5.5328$, $\frac{q}{\sqrt{|p||\mu|}} = 0.111$ which does not satisfy the necessary and sufficient condition given in Lemma 2. Thus the system cannot achieve consensus, and the curves of $\widehat{\xi}$ and ζ are shown in Fig. 4(a) and Fig. 4(b), respectively. This simulation verifies our conclusion that building connection regardless of the Veteran Rule may lead formation unstability.

Another of our simulation in Fig. 5 further shows the effectiveness of the Veteran Rule that the system still achieves formation stability when the scale of the formation goes very large (with 600 UAVs).

5.2 Convergence Rate

We use a similar setting in the $10 + 2$ UAV formation example in Section 5.1 to analyze the optimal convergence rate, and the only difference is the control parameter $\gamma = 0.5$. From Theorem 2, we know that the optimal in-degree for each UAV is $\frac{4}{\gamma^2} = 16$. We assume all the 10 UAVs in the original formation system chose this optimal in-degree, and see how the convergence rate β^* changes when UAVs 11 and 12 vary their in-degrees from 10 to 20 (see Fig. 6). From Fig. 6 we can observe that the convergence rate reaches its maximum value when the in-degrees of UAVs 11 and 12 are equal to $\frac{4}{\gamma^2} = 16$, which corroborates the result in Theorem 2.

In Fig. 7, we show the velocity curves (w.r.t. y-axis) of the

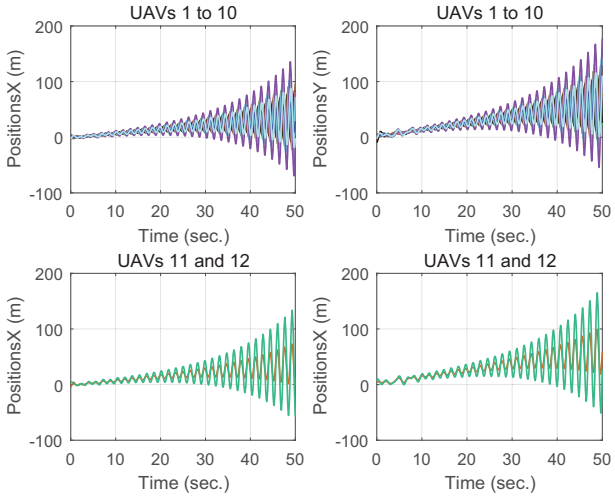

(a)

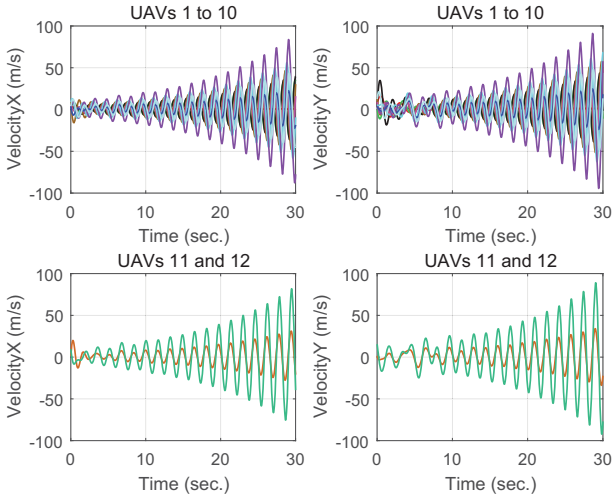

(b)

Fig. 4: Two new UAVs join in the system without using the Veteran Rule, and the system diverges. (a) Position response of the system; (b) Velocity response of the system.

two new UAVs under two randomly given in-degrees (i.e., μ_1 and μ_3) and the optimal in-degree μ_2. We can see that the curves under μ_2 converge faster than under μ_1 and μ_3.

6 Conclusion

In this paper, the scalability problem has been studied for UAV formation systems governed by double-integrator dynamics. Inspired from pigeon flocks, we have proposed the Veteran Rule to solve this problem under fixed control parameters. Furthermore, the convergence rate of the formation system under the proposed Veteran Rule has been analyzed. Counterintuitively, we found that the optimal convergence rate require all the in-degrees to equal $\frac{4}{\gamma^2}$, where γ is the control parameter; and any additional in-degrees do not contribute to the convergence rate, but have negative effects. Based on this result, the Veteran Rule with optimal convergence rate has been designed. Simulation results have shown the effectiveness of our theory and design.

References

[1] (2018) Integration of civil unmanned aircraft systems (uas) in the national airspace system (nas) roadmap.

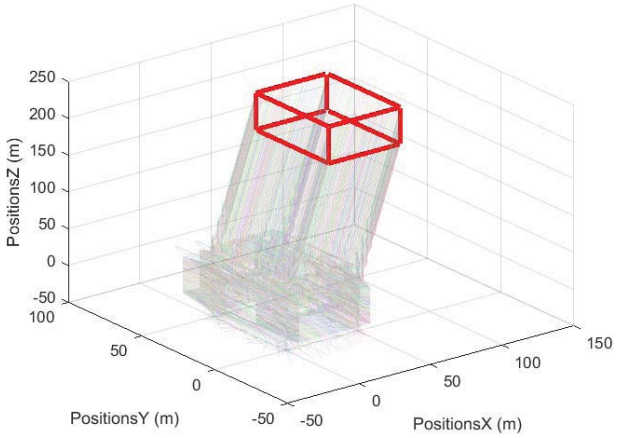

Fig. 5: A formation system with 600 UAVs using the Veteran Rule, where the formation pattern is a $50 \times 50 \times 50$ cube.

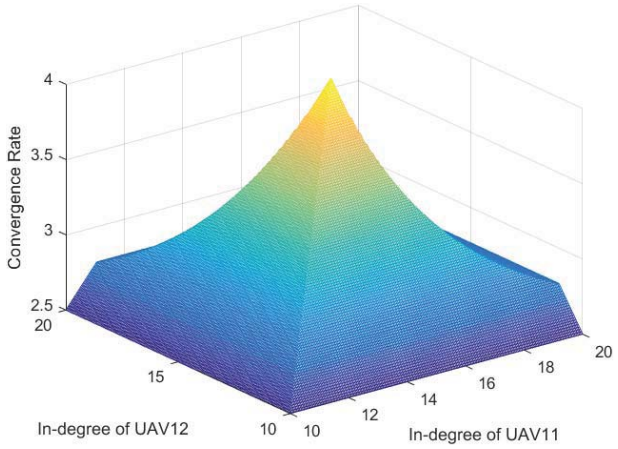

Fig. 6: The convergence rate w.r.t. the in-degrees of the two new UAVs.

[2] (2017) Unmanned systems integrated roadmap 2017-2042.

[3] Y. Cao, W. Yu, W. Ren, and G. Chen, "An overview of recent progress in the study of distributed multi-agent coordination," *IEEE Trans. Ind. Informat*, vol. 9, no. 1, pp. 427–438, Feb. 2013.

[4] X. Wang, Z. Zeng, and Y. Cong, "Multi-agent distributed coordination control: Developments and directions via graph viewpoint," *Neurocomputing*, vol. 199, pp. 204 – 218, Jul. 2016.

[5] B. D. Anderson, B. Fidan, C. Yu, and D. Walle, "Uav formation control: Theory and application," vol. 371, no. 3, pp. 15–33, Mar. 2008.

[6] X. Dong, B. Yu, Z. Shi, and Y. Zhong, "Time-varying formation control for unmanned aerial vehicles: Theories and applications," *IEEE Trans. Control Syst. Technol*, vol. 23, no. 1, pp. 340–348, Apr. 2015.

[7] Z. Li, Z. Duan, G. Chen, and L. Huang, "Consensus of multiagent systems and synchronization of complex networks: A unified viewpoint," *IEEE Trans. Circuits Syst. I, Reg. Papers*, vol. 57, no. 1, pp. 213–224, Jun. 2010.

[8] Z. Li, Z. Duan, and G. Chen, "Dynamic consensus of linear multi-agent systems," *IET Control Theory Appl.*, vol. 5, no. 1, pp. 19–28, Jan. 2011.

[9] W. Ren, "On consensus algorithms for double-integrator dynamics," *IEEE Trans. Autom. Control*, vol. 6, no. 53, pp. 1503–1509, 2008.

[10] J. Qin and C. Yu, "Cluster consensus control of generic lin-

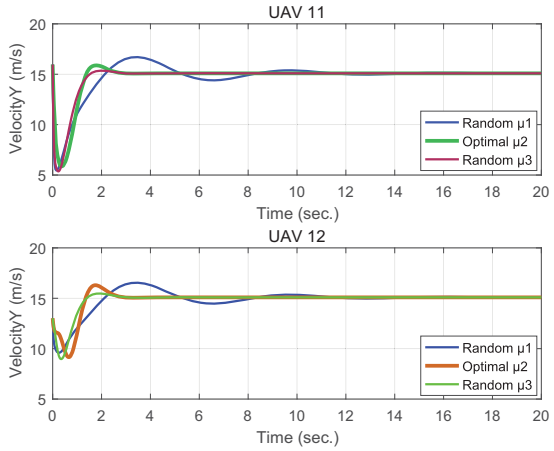

Fig. 7: The y-direction velocity curves under the optimal in-degree and two randomly given in-degrees.

ear multi-agent systems under directed topology with acyclic partition," *Automatica*, vol. 49, no. 9, pp. 2898–2905, Sept. 2013.

[11] Z. Li, W. Ren, X. Liu, and L. Xie, "Distributed consensus of linear multi-agent systems with adaptive dynamic protocols," *Automatica*, vol. 49, no. 7, pp. 1986–1995, Jul. 2013.

[12] Z. Li, W. Ren, X. Liu, and M. Fu, "Consensus of multi-agent systems with general linear and lipschitz nonlinear dynamics using distributed adaptive protocols," *IEEE Trans. Autom. Control*, vol. 58, no. 7, pp. 1786–1791, Dec. 2013.

[13] Z. Li, G. Wen, Z. Duan, and W. Ren, "Designing fully distributed consensus protocols for linear multi-agent systems with directed graphs," *IEEE Trans. Autom. Control*, vol. 60, no. 4, pp. 1152–1157, Apr. 2015.

[14] F. Muñoz, E. S. Espinoza Quesada, H. M. La, S. Salazar, S. Commuri, and L. R. Garcia Carrillo, "Adaptive consensus algorithms for real-time operation of multi-agent systems affected by switching network events," *Int. J. Robust Nonlin. Control*, vol. 27, no. 9, pp. 1566–1588, Oct. 2017.

[15] H. Yu and X. Xia, "Adaptive consensus of multi-agents in networks with jointly connected topologies," *Automatica*, vol. 48, no. 8, pp. 1783–1790, Aug. 2012.

[16] J. Xi, N. Cai, and Y. Zhong, "Consensus problems for high-order linear time-invariant swarm systems," *Phys. A, Stat. Mech. Appl.*, vol. 389, no. 24, pp. 5619 – 5627, Dec. 2010.

[17] R. Olfati-Saber and R. M. Murray, "Consensus problems in networks of agents with switching topology and time-delays," *IEEE Trans. Autom. Control*, vol. 49, no. 9, pp. 1520–1533, Sept. 2004.

[18] M. Vidyasagar, *Nonlinear systems analysis*. Siam, 2002, vol. 42.

[19] W. Yu, G. Chen, and M. Cao, "Some necessary and sufficient conditions for second-order consensus in multi-agent dynamical systems," *Automatica*, vol. 46, no. 6, pp. 1089–1095, Jun. 2010.

[20] I. Watts, B. Pettit, M. Nagy, T. B. de Perera, and D. Biro, "Lack of experience-based stratification in homing pigeon leadership hierarchies," *R. Soc. Open Sci.*, vol. 3, no. 1, p. 150518, Jan. 2016.

[21] B. Pettit, Z. kos, T. Vicsek, and D. Biro, "Speed determines leadership and leadership determines learning during pigeon flocking," *Curr. Biol.*, vol. 25, no. 23, pp. 3132 – 3137, Oct. 2015.

[22] M. Nagy, Z. Akos, D. Biro, and T. Vicsek, "Hierarchical group dynamics in pigeon flocks," *Nature*, vol. 464, no. 7290, p. 890, Apr. 2010.

[23] P. E. Jorge and P. A. Marques, "Decision-making in pigeon flocks: a democratic view of leadership," *J. Exp. Biol.*, vol. 215, no. 14, pp. 2414–2417, Jun. 2012.

[24] C. D. Santos, S. Neupert, H.-P. Lipp, M. Wikelski, and D. K. Dechmann, "Temporal and contextual consistency of leadership in homing pigeon flocks," *PloS one*, vol. 9, no. 7, p. e102771, Jul. 2014.